PROCEEDINGS B

royalsocietypublishing.org/journal/rspb

Research

Synchrotron data reveal nautiloid characters in *Pohlsepia mazonensis*, refuting a Palaeozoic origin for octobrachians

Thomas Clements[1,2], Imran Alexander Rahman[3,4], Alan R. T. Spencer[3,5], Christian Klug[6], Dirk Fuchs[7], Isabelle Rouget[8], Isabelle Kruta[8], Sebastian Schöder[9], Jack Wittry[10], Orla G. Bath Enright[11,12] and Pierre Gueriau[13,14]

[1]School of Geography, Geology and the Environment, University of Leicester, Leicester, UK
[2]Department of Ecology and Evolutionary Biology, School of Biological Sciences, University of Reading, Reading, UK
[3]Natural History Museum, London, UK
[4]Oxford University Museum of Natural History, Oxford, UK
[5]Department of Earth Science & Engineering, Imperial College London, London, UK
[6]Paläontologisches Institut und Museum, Universität Zürich, Zürich, Switzerland
[7]Bayerische Staatssammlung für Paläontologie und Geologie, Munich, Bayern, Germany
[8]Centre de Recherche en Paléontologie—Paris (CR2P), Muséum National d'Histoire Naturelle, Paris, Île-de-France, France
[9]Synchrotron SOLEIL, L'Orme des merisiers, Saint-Aubin, France
[10]Field Museum of Natural History, Chicago, IL, USA
[11]Staatliches Museum für Naturkunde Stuttgart, Stuttgart, Germany
[12]School of the Environment and Life Sciences, University of Portsmouth, Burnaby Road, Portsmouth, UK
[13]Institute of Earth Sciences, Université de Lausanne, Lausanne, Switzerland
[14]Ministère de la Culture, Université Paris-Saclay, Gif-sur-Yvette, France

TC, 0000-0002-6563-4720; IAR, 0000-0001-6598-6534; ARTS, 0000-0001-6590-405X; CK, 0000-0002-4099-7453; DF, 0000-0003-0648-1231; IR, 0000-0002-9673-0416; IK, 0000-0002-4485-541X; OGBE, 0000-0002-0341-6402; PG, 0000-0002-7529-3456

Pohlsepia mazonensis, from the late Carboniferous Mazon Creek Lagerstätte (311–306 Ma), has been suggested to be the oldest fossil octopus. This single specimen provides a key calibration point for molecular clock studies, which estimated a Palaeozoic origin for octobrachians, pushing the fossil record of crown octopuses back 150 million years. Despite being a textbook 'phylogenetic fuse' example, the systematic position of *Pohlsepia* is controversial and, consequently, our understanding of cephalopod evolution remains in flux. We present the first comprehensive reassessment of this enigmatic fossil, alongside multiple new specimens, using a suite of advanced analytical techniques. Synchrotron micro-X-ray fluorescence elemental mapping reveals a radula obscured by the matrix, definitively confirming a molluscan affinity. Crucially, radular tooth count and morphology indicate that *Pohlsepia* is not an early octobrachian but rather a decomposed nautiloid. This reinterpretation refutes a Palaeozoic origin for octobrachians and provides the only unequivocal evidence of nautiloid soft tissue in the Palaeozoic fossil record. Our findings demonstrate how advanced analytical methods can be used to resolve the interpretive challenges posed by the exceptional but often ambiguous soft tissue preservation in the Mazon Creek Lagerstätte, offering great potential for the re-evaluation of other fossil specimens from this iconic site.

Cite this article: Clements T *et al*. 2026 Synchrotron data reveal nautiloid characters in *Pohlsepia mazonensis*, refuting a Palaeozoic origin for octobrachians. *Proc. R. Soc. B* **293** : 20252369.
https://doi.org/10.1098/rspb.2025.2369

Received: 12 September 2025
Accepted: 11 February 2026

Subject Category:
Palaeobiology

Subject Areas:
palaeontology, evolution

Keywords:
octopus, taphonomy, fossil, Mazon Creek, decay, cephalopod, Nautilus

Author for correspondence:
Thomas Clements
e-mail: clements.taph@gmail.com

Electronic supplementary material is available online at https://doi.org/10.6084/m9.figshare.c.8388504.

THE ROYAL SOCIETY
PUBLISHING

1. Introduction

Described in 2000 from a solitary siderite concretion, *Pohlsepia mazonensis* [1] (figure 1*a,b*) fundamentally challenged our understanding of cephalopod evolution when it was interpreted as the oldest known octopus, predating previous estimates by over 150 million years. This charismatic but contentious fossil from the late Carboniferous Mazon Creek Lagerstätte (311–306 Ma) [5] was described as possessing a distinctive 'sac-like' fused head and mantle, symmetrical fins, paired eyespots and arm crown with both arms and specialized tentacles, while at the same time lacking any evidence of an internal or external shell (figure 1*c*). Based on this combination of characteristics, Kluessendorf and Doyle [1] interpreted *P. mazonensis* as a cirrate octopod, a member of a group of 'primitive' benthic octopods that inhabit present-day deep-water marine environments (e.g. [6,7].

The identification of a crown cirrate octopod in the Carboniferous dramatically reconfigured the timeline of cephalopod evolution. Prior to Kluessendorf & Doyle [1], crown coleoids (octopus, cuttlefish and squid) were thought to have diverged in the Jurassic (e.g. [8]). However, the description of *P. mazonensis* pushed the origin of octobrachians—and by extension the split between Octobrachia and Decabrachia—deep into the Palaeozoic [1,9] (figure 1*g*). This single fossil anchored subsequent molecular divergence time estimates, serving as the primary calibration point in many of the first cephalopod phylogenetic studies, all of which inferred Palaeozoic origins for major coleoid lineages (e.g. [10–12]). Building upon these findings, the presence of a derived octopod in the Palaeozoic has been used as a textbook example of a 'phylogenetic fuse' (i.e. where a single fossil implies a much longer evolutionary history than previously recognized; see [13,14]) and was evidenced as a justification for a coleoid affinity for enigmatic Cambrian fossils, such as the highly controversial *Nectocaris pteryx* (e.g. [15,16]; see also [17]).

The placement of *P. mazonensis* as a crown cirrate octopus is, however, controversial. Many of the purported 'octopode' characters identified by Kluessendorf & Doyle [1]—including the arm crown, fins and funnel—are highly contentious [18,19], and the fossil lacks key cirrate features such as an internal shell vestige, single row of suckers and arm cirri [20–22]. Even seemingly unequivocal anatomical characters have come under scrutiny: Rogers *et al*. [23] examined the paired 'eyespot' structures, finding no evidence of melanosomes, the characteristic melanin synthesizing organelles observed in extant and extinct coleoid eyes. This is unusual; melanosomes readily preserve in Mazon Creek fossils [24–27]. Additionally, Rogers *et al*. [23] found that the chemical signatures of the paired structures do not resolve with the chemical signatures of other coleoid cephalopod ocular pigments, further undermining their octopod affinity. Indeed, Sutton *et al*. [28] failed to phylogenetically resolve *P. mazonensis* among crown octopodiformes, instead placing it as a basal coleoid with 'uncertain affinities', while the morphological uncertainties have led other researchers to question whether *P. mazonensis* represents a cephalopod [2,29] or even a mollusc [30,31]. Unsurprisingly, when *P. mazonensis* is excluded from molecular clock analyses, studies consistently support a Mesozoic origin for crown Octobrachia [2–4,32]. This timing aligns well with the earliest unequivocal fossil evidence of crown octopods from the late Jurassic ([33,34] see figure 1*g*) as well as the excellent fossil record documenting internal shell reduction in stem-octopods, a process that ultimately led to the reduced shell character states observed in extant cirrates (e.g. [33,34]).

Comprehensive reassessment of *P. mazonensis* is of timely importance yet is a challenging prospect; our understanding of soft-tissue preservation mechanisms in siderite concretions remains limited (e.g. [5]) making definitive morphological interpretation from a single ambiguous soft tissue specimen particularly problematic without new anatomical character complexes (e.g. [25]). Typically, soft tissues from the Mazon Creek Lagerstätte are preserved as 2D light-on-dark 'stains' associated with minimal mouldic relief [5,35]. Kluessendorf & Doyle [1] acknowledged the difficulty interpreting the soft tissue anatomy of *P. mazonensis* based on the colouration of the matrix—this challenge is typified by the cryptic light stains that protrude from the main body of *P. mazonensis*, which were ultimately dismissed by Kluessendorf & Doyle [1] as non-biological '*fluids expressed from the animal after burial*'. It is fair to say that the morphological ambiguity of *P. mazonensis'* soft tissues clouds the systematic placement of this iconic fossil.

In this study, we present a much-needed reassessment of *P. mazonensis*, alongside an investigation of several other previously undescribed soft tissue Mazon Creek specimens that are visually similar to *P. mazonensis*, using a suite of analytical and imaging techniques. By reevaluating this controversial fossil that has shaped cephalopod evolutionary timelines for over two decades and presenting new anatomical characters, we contribute new perspectives to the ongoing discussion about the timing of major cephalopod radiations and the reliability of evolutionary narratives based on ambiguous soft-bodied fossils.

2. Material and methods

(a) Fossil specimens and updated locality data

The focus of this study is the single specimen of *P. mazonensis* from the Mazon Creek Lagerstätte, consisting of a part (FMNH PE51727a; figure 1*a*) and counterpart (FMNH PE51727b; figure 1*b*; a video of the specimen can be seen in the electronic supplementary material). During the course of our investigations, we were made aware of several additional Mazon Creek fossils that looked visually similar to *P. mazonensis*, which have been tentatively identified as cf. *Paleocadmus*? based on the presence of mouthparts/radulae: FMNH PE29383 (figure 1*d*), FMNH PE32522 (figure 1*e*), FMNH PE88991 (figure 1*f*; part and counterparts: electronic supplementary material, figure S1; mouthparts: electronic supplementary material, figure S6). These fossils were also investigated. All specimens are accessioned at the Field Museum of Natural History, Chicago, USA (FMNH).

P. mazonensis, and the other specimens examined herein, are each preserved within a siderite (iron carbonate) concretion found in the ex-coal strip mine, Pit 11 (Will and Kankakee counties, Illinois, USA [1]). Detailed geographic and stratigraphic data are lacking for where *P. mazonensis* was found—an issue when considering that Pit 11 is geographically large, covering

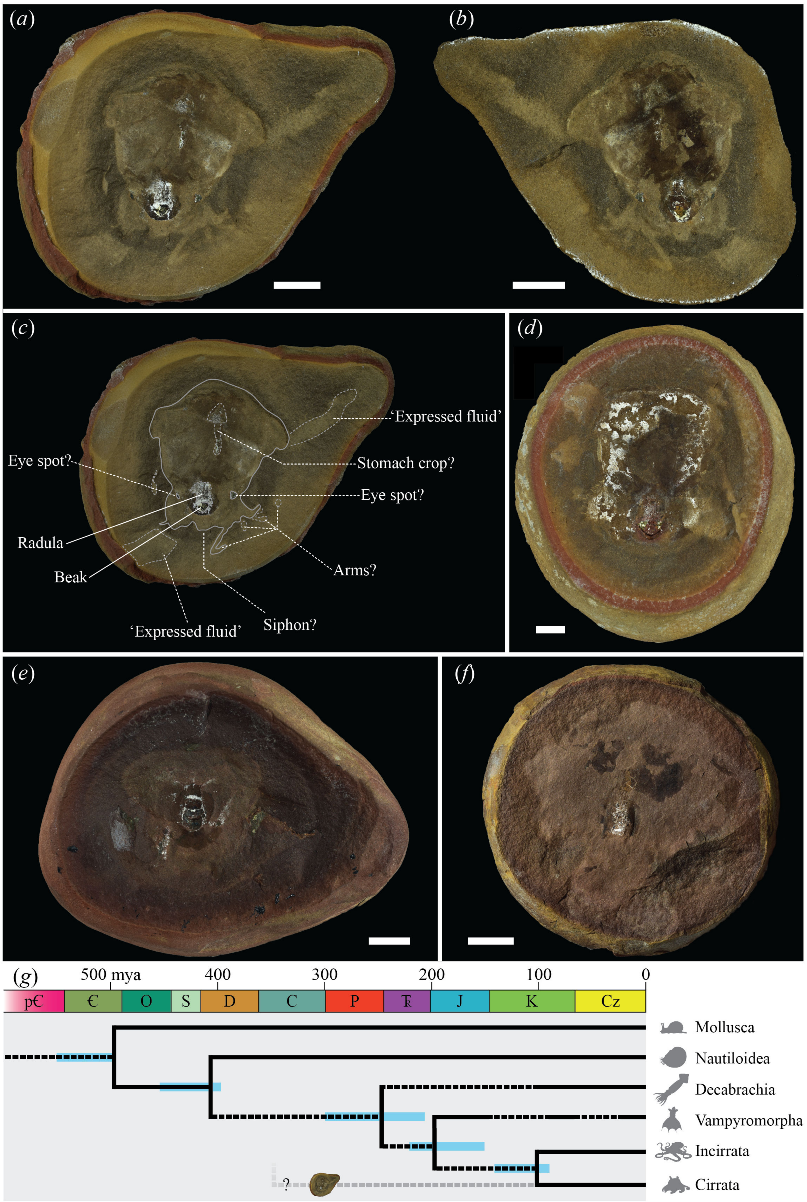

Figure 1. The fossils and soft tissue anatomy of *Pohlsepia mazonensis* and cf. Paleocadmus sp. (*a*) *Pohlsepia mazonensis* PE51727a (part). (*b*) *Pohlsepia mazonensis* PE51727b (counterpart). (*c*) The putative anatomy of *Pohlsepia mazonensis* (PE51727a). Dotted lines represent unresolved anatomical characters, and solid lines represent unambiguous anatomical characters identified in this study. (*d*) *cf. Paleocadmus sp*. (PE29383). (*e*) *cf. Paleocadmus sp*. (PE32522). (*f*) *cf. Paleocadmus* sp. (PE88991). Scales: 1 cm. All *Paleocadmus* samples (parts and counterparts) can be seen in electronic supplementary material, figure S1. (*g*) A schematic of a molecularly calibrated time-tree of cephalopod evolution with solid lines indicating known fossil occurrences. Blue squares indicate molecular divergence data based on Kröger *et al*. [2], Tanner *et al*. [3] and López-Córdova *et al*. [4]. The putative position of *Pohlsepia* as a cirrate is marked, demonstrating the conflict of a highly derived crown-group octopus existing 150 million years before the transitional octopus fossils of the Mesozoic.

approximately 14 km^2. We can deduce that *P. mazonensis* was extracted from the lower 3 to 8 m section of the Francis Creek Shale Member, as this is the fossiliferous part of the section associated with the Mazon Creek Lagerstätte biota (see [5] for a review of the Lagerstätte), although it is unclear whether *P. mazonensis* was found *in situ* or as part of the spoil heaps that were historically picked over by collectors (e.g. [36]).

The fossiliferous sub-section of the Francis Creek Shale Member represents the voluminous deposition of terrestrially derived, iron-rich, riverine muds and silts into a tidally influenced brackish marine basin [5,35]. This large discharge of water and sediment transported allochthonous terrestrial plants and organisms into the bay, burying them and smothering native marine organisms in an extensive sediment fan (although it is unclear if the high sedimentation rates or freshwater input acted as the kill mechanism [5]). The inundating sediments, with their high iron content, created the geochemical conditions required for the precipitation of authigenic siderite to form around the decaying soft tissues, geologically stabilizing them within concretions. The exact controls and mechanisms of this type of soft tissue preservation are still being investigated (for reviews see [5,35]). In the marine areas of the Mazon Creek Lagerstätte, such Pit 11, a diverse range of ecto- and endocochleate cephalopods have been described although they are numerically rare compared to other animal groups [37,38].

(b) Scanning electron microscope energy dispersive spectroscopy

PE51727 was investigated using a Hitachi TM4000Plus scanning electron microscope (SEM), Imperial College, UK, with backscattered electron images collected at an accelerating voltage of 15 kV. Energy dispersive spectroscopy (EDXS) was used for semi-quantitative analyses using an Oxford Instruments AZtec series silicon drift detector with an energy resolution of 151 eV (Cu-Ka; at an accelerating voltage of 15 kV with no gain calibration). Oxford instruments matrix corrections were used against factory standards.

(c) Micro-CT scanning

PE51727 was micro-CT scanned using a Nikon XT H 225 cabinet scanner, University of Bristol, UK. The part was scanned with a 1 mm thick copper filter, 222 kV voltage, 203 μA current and 3142 projections (each with an exposure time of 500 ms), while the counterpart was scanned with a 1 mm thick copper filter, 222 kV voltage, 188 μA current and 3142 projections (each with an exposure time of 708 ms). These scans were digitally reconstructed as three-dimensional computer models using the SPIERS software suite [39].

(d) Synchrotron analysis

Synchrotron micro-X-ray fluorescence (μXRF) major-to-trace elemental mapping was performed on PE51727 and PE29383 at the PUMA beamline of the SOLEIL synchrotron source, France [40], using a 18.5 keV monochromatic beam, which was selected for excitation of K-lines from phosphorus to zirconium and L-lines from cadmium to uranium. The incoming X-ray beam was focused using Kirkpatrick-Baez mirrors to a spot size of approximately 7 × 5 μm^2 (H × V, full width at half maximum). The sample was mounted on a scanner stage allowing 150 mm and 100 mm movements (in horizontal and vertical directions, respectively) with sub-micrometre accuracy, and orientated at 45° to the incident beam, producing an effective beam size of approximately 10 × 5 μm^2 (H × V) on the sample. XRF was collected using a SiriusSD silicon drift detector (SGX Sensortech Ltd, 100 mm^2 active area) orientated at 90° to the incident beam, in the horizontal plane. Two-dimensional spectral images, i.e. images for which each pixel is characterized by a full XRF spectrum, were collected on the fly [41] over the specimens at a 25–80 μm lateral resolution with a 40–50 ms dwell time (effective counting time was 90% of the dwell time) depending on the samples (acquisition parameters are given in figure captions). All the elemental distributions presented herein correspond to integrated intensities from the main XRF peaks, represented using logarithmic colour or linear grey scales that go from dark to light for low to high intensities, respectively.

(e) Multispectral imaging

PE51727 and PE29383 were investigated using multispectral imaging at the IPANEMA laboratory, Gif-sur-Yvette, France. Building on the concept of UV photography [42] and visible light fluorescence imaging [43–45], reflection and luminescence images in various spectral ranges were collected using a setup consisting of a low-noise 4.2-megapixel CMOS camera (ORCA-Flash4.0 LT PLUS, Hamamatsu) with high sensitivity from 350 to 900 nm, fitted with a UV–VIS–IR 60 mm 1 : 4 Apo Macro lens (CoastalOptics), in front of which was positioned a filter wheel holding eight interference band-pass filters (Semrock) to collect images in eight spectral ranges from 472 to 935 nm. Illumination was provided by 16 LED lights ranging from 365 to 700 nm wavelength (CoolLED pE-4000), coupled to a liquid light-guide fitted with a fibre-optic ring light-guide. As such, more than 90 different illumination/detection couples were available, and the resulting greyscale images were combined into false colour RGB images to enhance morphological contrasts or reveal details invisible in traditional photography using only visible light. Image stacking, image registration of the different couples and production of false colour RGB composites were performed in ImageJ. Acquisition parameters: lateral scanning step, 80 μm; dwell time, 40 ms (figure 2e,f).

3. Results and discussion

(a) Soft tissues and body outline

Synchrotron micro-X-ray fluorescence, SEM EDXS and multispectral imaging were used to re-investigate the contentious soft tissue anatomical characters of *P. mazonensis* (figure 2). SEM EDXS mapping shows a slight elevation in the clay content, especially kaolinite, in the white stain that represents the main body of the animal compared to the matrix (electronic supplementary material, figures S2a–I and S3a–d). Similarly, synchrotron micro-X-ray fluorescence elemental mapping shows that the body stain is enriched in copper and arsenic compared to the surrounding concretionary matrix. We did not observe any elevation of clays, copper and arsenic, in the ‘expressed fluid’ (figure 2*c*,*d*). Despite looking visually similar to the body stain, our data indicate that these discolorations of the matrix are unlikely to be a true soft tissue anatomical character—confirming the original assessment of Kluessendorf and Doyle [1]. This structure could be taphonomic fluids that leaked from the carcass, although we speculate that it could perhaps represent a burrow that was captured and preserved during the formation of the siderite concretion, but we cannot confirm this. Regardless, our results here show that identifying enigmatic soft tissues via

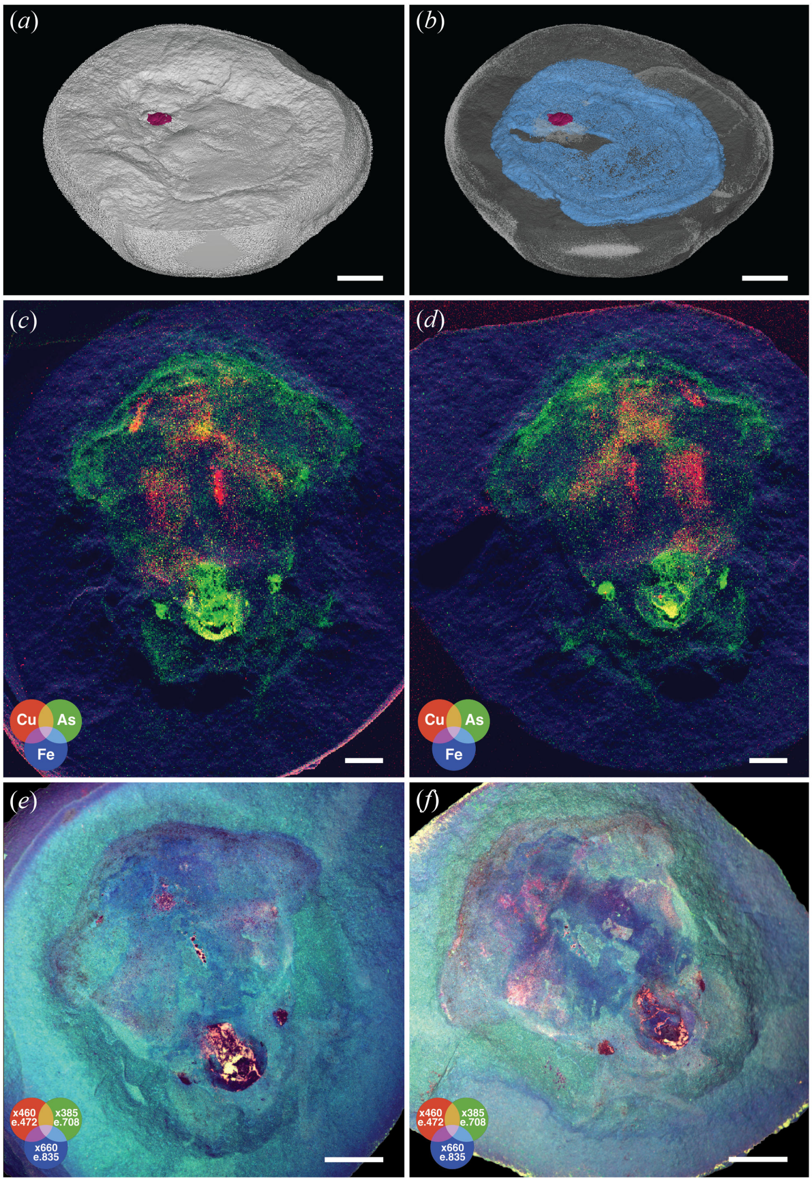

Figure 2. Analytical investigations of *Pohlsepia mazonensis* (*PE51727*). (*a*) Virtual reconstruction based on micro-CT showing the external concretionary surface of PE51727a. Mouthparts are highlighted in purple. (*b*) Virtual reconstruction based on micro-CT with the external surface of PE51727a partly transparent. Mouthparts are highlighted in purple and the area of high X-ray attenuation is shown in blue. (*c*) Synchrotron micro-X-ray fluorescence (µXRF) elemental map of PE51727a showing copper (red), arsenic (yellow) and iron (blue). (*d*) Synchrotron micro-X-ray fluorescence (µXRF) elemental map of PE51727b showing copper (red), arsenic (yellow) and iron (blue). (*e*,*f*) Multispectral false colour RGB images of PE51727a (*e*) and PE51727b (*f*). Illumination/detection couples used: red—illum. 460 nm/det. 472 ± 15 nm (reflection), green—illum. 385 nm/det. 708 ± 37 nm (luminescence), blue—illum. 660 nm/det. 835 ± 35 nm (lum.). Scales: 1 cm.

visual colour changes in the concretionary matrix alone is not advisable. We advise, where possible, using multiple lines of analytical investigation to resolve enigmatic soft tissues in the exceptional fossils of the Mazon Creek Lagerstätte.

Our analyses of the putative soft tissue characters of *P. mazonensis* allow us to conclude the following. (i) We find no tissue folds or a distinct funnel-like opening structure that confirms the presence of a siphon (electronic supplementary material, figure S2I). (ii) While the elemental maps and multispectral images do show some poorly preserved appendage-like structures (figure 2*c*–*f*; electronic supplementary material, figure S2g,i), we find limited evidence to support the presence of eight distinct arms or any specialized tentacles, as previously inferred by Kluessendorf & Doyle [1]. Similarly, none of the cf. *Paleocadmus* specimens we studied had distinguishable arm crowns or provided clear evidence of specialized armature. Moreover, micro-CT scanning of the 'arms' reveals no evidence of biomineralized arm hooks (figure 2*a*,*b*), which are known to preserve in the Mazon Creek [46]. (iii) Elemental maps confirm that the lobate 'fins' are part of the body outline (figure 2*c*,*d*; electronic supplementary material, figure S2D). Neither the elemental maps, multispectral images, nor visual investigations revealed any clear indicators of tissue folding or any definitive fin-like structures in *P. mazonensis* or any of the other *Paleocadmus* specimens. (iv) SEM EDXS investigation of the ink sack/stomach/crop revealed a three-dimensional structure infilled with pyrite and enriched in clays (figure 2c,d; electronic supplementary material, figure S2e,f). Importantly, no defining anatomical structures or evidence of melanosomes were observed, casting serious doubts on the interpretation of this structure as an ink sack. None of the other cf. *Paleocadmus* specimens we investigated have a similar structure (electronic supplementary material, figure S1). (v) The paired 'eyespots' consist of three-dimensional shallow bowl-like impressions infilled with a darker stained matrix. The dark stain is characterized by elevated levels of pyrite and kaolinite (electronic supplementary material, figure S2b,c and S3b); however, we could not identify any melanosomes or impressions of melanosomes. Eyespot-like structures are also present in cf. *Paleocadmus*; they are visible in PE32522 (electronic supplementary material, figure S6d) and a singular 'eyespot' that is not visible to the naked eye was detected in PE29383 with synchrotron mapping (electronic supplementary material, figure S5). These structures are morphologically similar to the shallow bowl-like structures of *P. mazonensis* and, likewise, had no identifiable melanosomes; their position and dimensions, however, coincide with where the animal's eyes would be expected (compare [47]).

Micro-CT scanning did not reveal any evidence of shell material within or on the surface of the *P. mazonensis*. However, a flattened circular area characterized by relatively high X-ray attenuation can be observed within the concretion (figure 2*b*). Based on overall shape, the structure does not appear to be biological in origin. Dense minerals, such as sphalerite and pyrite, are commonly known to form during late-stage concretion formation in the Mazon Creek Lagerstätte [5,35]. Interestingly, an elongate 'void' in the dense material is visible below the mouthparts—this is not a true 'void' but rather the original siderite matrix. This structure does not appear to be biological but occurs along a crack within the concretion. This could be a septarian fracture (e.g. [5]), however, without sectioning the concretion, it is impossible to accurately determine either the dense material or the void structure at this time.

(b) Radula

Synchrotron μ-XRF analysis revealed a previously undetected morphological character that represents the only unequivocal anatomical character with systematic implications in *P. mazonensis*. When undertaking Fe mapping of the buccal area, no elemental contrast was observed between the fossil remains and the siderite, but the high Fe content, together with the sharpness of μ-XRF mapping and limited depth probed (attenuation length of Fe in siderite is ca. 30 μm), provided a high-resolution surface scan of the fossil revealing the presence of a previously unobservable radula and beak-like mandibles in close proximity to the presumed arm crown (figure 3). The presence of a radula confirms that *P. mazonensis* is a mollusc. Both upper and lower beaks appear to be preserved in an anterior/posterior orientation. The beak elements are incomplete, with both the rostrum tips and wings broken (possibly during splitting of the concretion). The radula is a shallow mouldic structure; it is unclear if any original material persists due to the presence of overlying matrix but based on other cephalopod and polyplacophoran radulae from the Mazon Creek, this is unlikely (e.g. [37,38,46,48,49]). The radula is incomplete; it is difficult to discern if the radula folds 'into' the concretion matrix or if it disarticulated during decay. Synchrotron μ-XRF analysis allows us to observe at least 11 distinct elements per transverse row: a central rachidian tooth (R), lateral teeth pairs (L1 and L2?), two pairs of marginal teeth (M1 and M2), and at least one pair of smooth marginal plates with no noticeable grooves (MP2) (figure 3*b–d*; reconstruction: figure 4*a*). The combination of the radula being laterally compressed and the resolution limitations of the scan meant that it was difficult to accurately resolve the morphology and exact size of each element, particularly the lateral teeth pairs, however we can confidently state that (i) the central rachidian tooth appears to consist of a central mesocone without any obvious flanking ectocones, (ii) the lateral teeth pairs are smaller in height than the central rachidian tooth but appear to have wider bases, (iii) the marginal teeth are larger than the lateral teeth and are curved with a unicuspid morphology, and (iv) the presence of at least one pair of marginal plates can be inferred based on the faint rectangular impressions observed on the right side of the radula (figure 3*c*). Our analyses further identify that multiple cf. *Paleocadmus* specimens also preserve with a radula and/or beaks (PE29383; PE32522; PE88991; electronic supplementary material, figures S1 and S5).

4. *Pohlsepia* is a nautiloid

The identification and configuration of the radula, alongside the general morphology of the teeth, unambiguously places *P. mazonensis* within Cephalopoda. Our analysis reveals at least 11 elements in each radula row—more than the 7 or 9 elements per transverse row seen in crown coleoids but less than the 13 elements seen in nautiloids [46,50]. Based on the number of elements and their general morphology, we can definitively reject a cirrate cephalopod affinity: while many extant cirrates have reduced or secondarily lost their radula as an adaptation to a deep-water habitats [7,54], genera including *Grimpoteuthis* [53], *Vampyroteuthis* [55] and *Luteuthis* [52] have a well-developed radula, consisting of 9 elements that are morphologically distinct from those seen *P. mazonensis* (figure 4*d–k*). This finding, alongside the clear morphological differences of the marginal plates, also allows us to reject a close relationship between *P. mazonensis* and the Mazon Creek coleoid *Saundersites illinoisiensis* (formerly *Jeletzkya douglassae* [46]; figure 4*c*; electronic supplementary material, figure S6).

Despite an incongruent element count, a nautiloid affinity for *P. mazonensis* is strongly supported by the following two lines of evidence. (i) The number of elements present in the radula of *P. mazonensis* is likely to be a preservational artefact. Compared to extant and extinct nautiloid radulae, *P. mazonensis* is missing a small pair of marginal plates (MP1) that typically sit behind the M2 elements (figure 4; electronic supplementary material, figure S4). Typically, MP1 elements are infrequently observed in Mazon Creek nautiloid radulae. The radulae of both *Paleocadmus herdinae* [48] and *Paleocadmus pohli* [37] are incompletely preserved—their radulae either fold into the concretion or show evidence of taphonomically related disarticulation (e.g. [48]). Typically, in these taxa MP1 are identified via composite reconstructions of the radula row by multiple specimens (e.g. [37]), which is not possible for the singleton *P. mazonensis*. Our scan does not have the resolution to allow us to identify MP1 elements, but we believe it is parsimonious that *P. mazonensis* did indeed have a pair of MP1 *in vivo* and, thus, a total of 13 elements. (ii) Our scan demonstrates that the radula of *P. mazonensis* is morphologically similar to that of the Mazon Creek nautiloid *P. pohli*. Both have a unicuspid central tooth, wide triangular lateral teeth and smooth elongate cresent-shaped marginal teeth [37] (figure 4*a*). We can discount an affinity to the other Mazon Creek nautiloid *Paleocadmus herdinae*—this radula has a weakly

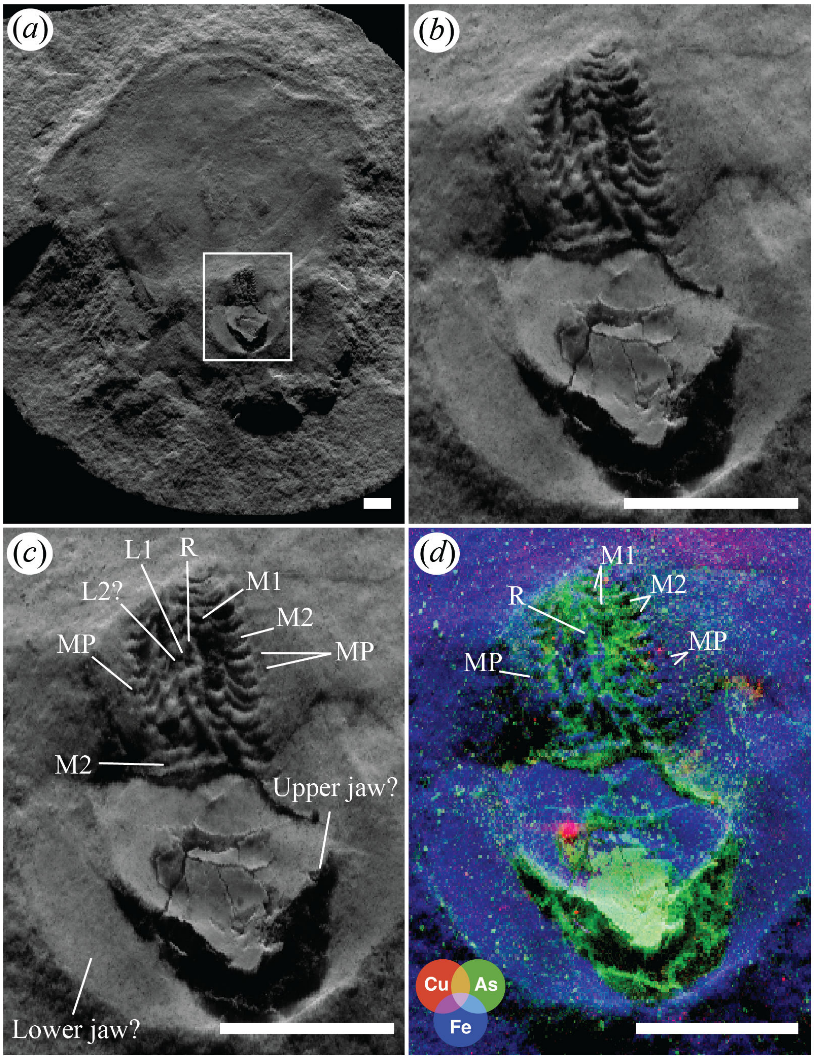

Figure 3. The radula and beak of *Pohlsepia mazonensis*. (*a*) Synchrotron micro-X-ray fluorescence (µXRF) iron (Fe) elemental map of PE51727a—the radula and beak region are marked by white box. Acquisition parameters: lateral scanning step, 80 µm; dwell time, 40 ms. (*b*) Increased magnification of the radula and beak region. (*c*) Annotated radula anatomy of *Pohlsepia mazonensis*. (*d*) Annotated synchrotron micro-X-ray fluorescence (µXRF) elemental map of PE51727a showing copper (red), arsenic (yellow) and iron (blue). Acquisition parameters: lateral scanning step, 25 µm; dwell time, 50 ms. Scales = 10 mm.

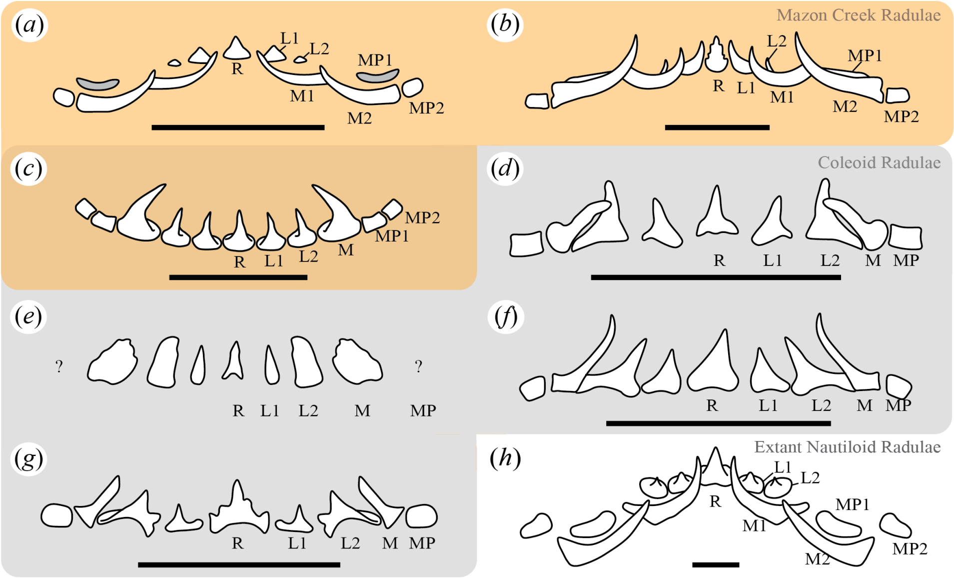

Figure 4. Radulae of extinct and extant cephalopods. (*a*) Composite reconstruction of *Paleocadmus pohli*'s radula row (from both fossil material and modified from [37,50]). The missing elements of PE51727 are marked in grey. (*b*) *Paleocadmus herdinae* (modified from [50]), (*c*) *Saundersites ilinoissensis* (modified from [46,50]), (*d*) *Vampyroteuthis infernalis* (modified from [51]), (*e*) *Luteuthis dentatus* (modified from [52]) (*f*) *Grimpoteuthis sp.*? (modified from [53]) (*g*) *Octopus vulgaris* (modified from [50]) and (*h*) *Nautilus pompilius* (modified from [50]). Abbreviations: R: rachidian tooth, L1: 1st lateral tooth, L2: 2nd lateral tooth, M1: 1st marginal tooth, M2: 1st marginal tooth. MP1: 1st marginal plate, MP2: 2nd marginal plate. Scale bars: 1 mm (scale missing = data unavailable).

tricuspid central tooth, elongated angular lateral teeth and marginal teeth with characteristic groove along the exterior [48] (figure 4*b*).

We therefore conclude that *P. mazonensis* (referred to as PE51727 from here) is certainly *Paleocadmus* sp. and based on the morphological evidence presented here, we determine that PE51727 is synonymous with, and by order of precedence should be referred to as, *P. pohli*. This reinterpretation has important implications for coleoid evolution: PE51727 and the *Paleocadmus* specimens represent the only unequivocal nautiloid soft tissue known from the Palaeozoic fossil record and thus the oldest by approximately 220 million years (e.g. [47]). Furthermore, as PE51727 is not a cirrate octopus, it now no longer conflicts with the body of evidence supporting the divergence of crown octopods during the late Jurassic (e.g. [2–4,33,34]). In turn, the lack of a crown cirrate in the late Carboniferous places serious doubt over a Palaeozoic origin for the major crown coleoid lineages and, in agreement with recent anatomical reassessments, demonstrates that a coleoid or even a cephalopod affinity for the highly controversial Cambrian fossil *N. pteryx* is not credible (per [2,17,56,57]). Lastly, our results confirm that PE51727 should not be used as a fossil calibration in studies investigating coleoid origins.

5. Systematics

Based on precedence, *P. mazonensis* (PE51727) is a junior synonym of *P. pohli*. We propose that, as the holotype of *P. pohli* (PE25583) consists of only an isolated radula, PE51727, with its soft tissues, should be considered the paratype.

Phylum MOLLUSCA
Class CEPHALOPODA Cuvier, 1797
Subclass NAUTILOIDEA Agassiz, 1847
Family is uncertain
Genus *Paleocadmus* Solen & Richardson, 1975
Paleocadmus pohli Saunders & Richardson, 1979

Synonymy. 2000 *Pohlsepia mazonensis* Kluessendorf & Doyle: 920, fig. 1.

Revised diagnosis. Small, soft-bodied nautiloid identified via radula impression consisting of 13 distinct elements per row. Teeth morphology: a relatively short, broadly triangular, unicuspid central rachidian tooth; wide triangular lateral teeth; elongate smooth crescent-shaped marginal teeth. Other anatomical characters include round body outline enriched in clays, incomplete beak, paired eye-like structures (shallow bowl-like impressions consisting of organic carbon and pyrite; possible preservation of decayed pin-hole eyes?), and incomplete arm crown with some evidence of tentacles. Shell currently unknown.

Holotype. PE25583 (isolated radula impression)

Paratype. PE51727 (body outline, various ambiguous soft tissues, radula impression and beak)

Occurrence: Francis Creek Shale Member, Illinois, USA (Mazon Creek Lagerstätte). Exact type locality unknown.

6. Taphonomy of a fossil nautiloid

Despite using a suite of analytical techniques, we find that interpreting the soft tissue anatomy of PE51727 remains challenging. We propose that the soft tissue anatomy of PE51727 and the *Paleocadmus* specimens are ambiguous because these organisms are in an advanced state of decay. Often the fidelity of preservation of body outlines and soft tissue anatomy in Mazon Creek fossils varies significantly within a single taxon, i.e. fossil specimens of the same taxon can be considered ‘taphomorphs’ (examples can be seen in [58,59]). This taphonomic variance has been hypothesized to be due to the depositional environment: in the ancient Mazon marine basin, recently deceased organisms were buried at varying rates depending on the sedimentary input, primarily controlled by distance from the palaeocoast [5,60]. Once buried, the rate of entombment by siderite, which would act to geologically stabilize the carcass, may have been variable due to environmental limiting variables, e.g. freshwater input, bioturbation, sedimentary Fe^{+} content, etc. [5,35]. Despite soft tissue preservation being common in the Mazon Creek Lagerstätte, these factors suggest that some carcasses may have undergone decay before becoming fossilized. The poor preservation of PE51727’s key anatomical soft tissue characters, such as the arm crown, limbs and the paired eyespots, indicates that the animal was in an advanced state of decay before geological stabilization. Determining how long PE51727 decayed for is difficult, especially as there are limited studies investigating the decay and disarticulation of soft tissues in extant *Nautilus* for direct comparison, however, based on the observation of beak/radula disarticulation during the decay of coleoid cephalopods, and assuming no scavengers caused the carcass to disarticulate, it could occur somewhere between a few days to a couple of weeks [61,62]. Regardless, the impact of decay makes interpretation of the body outline challenging, with one of the main ambiguous structures being the ‘fins’. In the *Paleocadmus* sp. specimens investigated (PE29383, PE32522; figure 1*d,e*), the ‘fins’ appear to be much more lobate and less well defined than the same structures in PE51727. We believe that a plausible alternative interpretation, based purely on visual morphology, is that the ‘fins’ could be decayed posterior cephalic retractor muscles and/or the digestive gland lobe structures seen in the soft tissue anatomy of extant nautiloids (electronic supplementary material, figure S4).

One interesting aspect of the Mazon Creek nautiloids is the lack of shell (conch); we are unable to ascertain whether PE51727 was buried with its shell. The flattened textural changes associated with the buccal mass of PE51727 suggest that the shell was impressed into the sediment surface before being detached. However, if the shell had been buried with the soft tissues, then it is likely that the shell, an impression, or a void left by shell dissolution, would have preserved (as seen in other nautiloid

Figure 5. Reconstruction of a *Paleocadmus* decaying prior to burial in the Mazon Creek marine basin. The separated shell is visible in the background. Other Mazon Creek fauna are visible, such as the polychaete *Esconites zelus* (foreground) and *Bandringa rayi*, an elasmobranch shark (back left). Palaeoart created by Franz Anthony.

and goniatitic ammonoid fossils described from the Mazon Creek Lagerstätte; see [38]). We found no direct evidence of shell material within PE51727 or (visually) on any of the other *Paleocadmus* specimens. It is possible that the advanced state of decay might provide the answer. Typically, the absence of preserved soft tissues in nautiloid fossils (and other ectocochleate cephalopods such as the ammonoids) is primarily prescribed to postmortem floating (e.g. [61,63–65]). In this scenario, the gas-filled chambered shell would float during decay, causing soft tissue fragments to disarticulate from the carcass, raining from the water column to the sediment surface. As the body outlines of the Mazon Creek nautiloids are relatively consistent, we deem this scenario unlikely. Recent investigations have shown that deceased modern *Nautilus* carcasses still associated with their shells can sink postmortem—if decay of the mantle and musculature allows the body shell chamber to become waterlogged [66]. Shell waterlogging neatly explains the presence of fossilized *in situ* jaws and stomach contents associated with fossilized ectocochleate cephalopod shells [67,68], however, two recent examples of shelled cephalopod soft tissues that have been identified without the corresponding shell [47,69] suggesting it is possible that the entire soft tissue anatomy could detach from the shell during decay. Whether this occurred in the water column or on the seafloor remains uncertain as does the precise timing of soft tissue separation from the shell; however, we believe that it is unlikely that soft tissues and the shells were buried together in PE51727 and the other *Paleocadmus* specimens (reconstructed in figure 5).

It should be noted that the preservation of nautiloid soft tissues is taphonomically atypical. Most soft tissue-bearing fossil coleoid cephalopods are preserved via the replacement of soft tissues by authigenic minerals such as apatite (calcium phosphate; phosphatization; [61,70,71]). In marine environments, apatite requires specific geochemical conditions to preferentially precipitate (e.g. [72]) but experiments have shown that the decay of carcasses typically generates adequate localized geochemical gradients to trigger mineralization [26,61,73]. However, experimental decay studies on coleoid cephalopods demonstrate that the use of ammonium-based buoyancy chemicals by Decabrachians reduces the intensity of the decay-induced geochemical gradients—creating a taxonomic bias that limits the preservation potential of these groups [61]. Clements *et al*. [61] suggested that the near absence of nautiloid, and ammonoid, soft tissues from the fossil record could be due to high levels of body tissue ammonia that could act to prevent diagenetic authigenic mineral replacement. The Mazon Creek Lagerstätte, however, does not preserve soft tissue directly via replacement by an authigenic mineral, but rather by the entombment of the carcass by iron carbonate (siderite). Experiments investigating siderite precipitation show that the nucleation phase occurs at higher pHs than phosphatization [74]. This may mitigate ammonia-related pH buffering that occurred during the decay of the nautiloids. Despite being incredibly rare in the context of the vast number of fossiliferous concretions known, the presence of multiple fossil nautiloids, as well as other soft-bodied cephalopods (e.g. *Saundersites illinoisiensis*), demonstrates that the sideritic concretionary mode of preservation of the Mazon Creek Lagerstätte is unusually suited for preserving ectocochleate cephalopods.

7. Conclusion

Our synchrotron micro-X-ray fluorescence elemental mapping analysis of *P. mazonensis* identified a previously unknown radula obscured by the concretionary matrix. The presence and morphology of the radular elements indicates that *P. mazonensis* does not represent a crown octobrachian but, in fact, represents the oldest known fossil soft tissue nautiloid (albeit without its shell). The reclassification of this enigmatic cephalopod refutes a Palaeozoic origin for octobrachians, lending further support to a mid/late Mesozoic origin for crown Octopoda, and further diminishing support for the dubious coleoid affinity of the controversial Cambrian soft-bodied fossil *N. pteryx*. Our findings highlight the interpretive difficulties when assessing the exceptional, yet occasionally ambiguous, soft tissue preservation seen in Mazon Creek Lagerstätte—emphasizing the need for rigorous re-evaluation when investigating enigmatic concretionary soft-bodied fossil material.

Ethics. This work did not require ethical approval from a human subject or animal welfare committee.

Data accessibility. XCT data are available on Dryad [75].

Supplementary material is available online [76].

Declaration of AI use. We have not used AI-assisted technologies in creating this article.

Authors' contributions. T.G.C.: conceptualization, data curation, formal analysis, funding acquisition, investigation, methodology, project administration, resources, supervision, validation, visualization, writing—original draft, writing—review and editing; I.A.R.: data curation, formal analysis, investigation, writing—review and editing; A.R.T.S.: data curation, formal analysis, investigation, writing—review and editing; C.K.: writing—review and editing; D.F.: writing—review and editing; I.R.: writing—review and editing; I.K.: writing—review and editing; S.S.: writing—review and editing; J.W.: resources, writing—review and editing; O.G.B.E.: investigation, writing—review and editing; P.G.: data curation, formal analysis, funding acquisition, investigation, writing—review and editing.

All authors gave final approval for publication and agreed to be held accountable for the work performed therein.

Conflict of interest declaration. We declare we have no competing interests.

Funding. No funding has been received for this article.

Acknowledgements. We would like to thank Christopher Rogers (University College Cork) for expert detective work locating and loaning *Pohlsepia* during the origins of this paper. Paul Mayer (FMNH) is thanked for collections support and loaning of sample material. Liz Martin (University of Bristol) and Jianguo Li (University of Birmingham) are thanked for operating analytical equipment. Palaeoart in figure 5 was created by Franz Anthony and images in electronic supplementary material, figure S4 supplied by Neil Landman. Amanda Clements, Juan Benito, Richard Dearden and Emma Dunne are thanked for constructive feedback. Three anonymous reviewers are thanked for their very positive and constructive feedback. We dedicate this paper to the memory of Dr Joanne Kluessendorf, a Mazon Creek cephalopod authority and original describer of *Pohlsepia*, who sadly passed away in 2018.

References

1. Kluessendorf J, Doyle P. 2000 *Pohlsepia mazonensis*, an early 'octopus' from the Carboniferous of Illinois, USA. *Palaeontology* **43**, 919–926. (doi:10.1111/1475-4983.00155)
2. Kröger B, Vinther J, Fuchs D. 2011 Cephalopod origin and evolution: a congruent picture emerging from fossils, development and molecules: extant cephalopods are younger than previously realised and were under major selection to become agile, shell-less predators. *BioEssays* **33**, 602–613. (doi:10.1002/bies.201100001)
3. Tanner AR *et al*. 2017 Molecular clocks indicate turnover and diversification of modern coleoid cephalopods during the mesozoic marine revolution. *Proc. R. Soc. B* **284**, 20162818. (doi:10.1098/rspb.2016.2818)
4. López-Córdova DA, Avaria-Llautureo J, Ulloa PM, Braid HE, Revell LJ, Fuchs D, Ibáñez CM. 2022 Mesozoic origin of coleoid cephalopods and their abrupt shifts of diversification patterns. *Mol. Phylogenetics Evol*. **166**, 107331. (doi:10.1016/j.ympev.2021.107331)
5. Clements T, Purnell M, Gabbott S. 2019 The Mazon Creek Lagerstätte: a diverse late Paleozoic ecosystem entombed within siderite concretions. *J. Geol. Soc*. **176**, 1–11. (doi:10.1144/jgs2018-088)
6. Grimpe G. 1916 *Chunioteuthis*-eine neue cephalopodengattung. *Zool. Anz.* **46**, 349–359.
7. Collins MA, Villanueva R. 2006 Taxonomy, ecology and behaviour of the cirrate octopods. In *Oceanography and marine biology: an annual review* (eds RN Gibson, RJA Atkinson, JDM Gordon), pp. 277–322, vol. **44**. London, UK: Taylor & Francis. (doi:10.1201/9781420006391.ch6)
8. Doyle P, Donovan DT, Nixon M. 1994 Phylogeny and systematics of the Coleoidea. *Univ. Kansas Paleontol. Contrib. (n.s.)* **5**, 1–15.
9. Doguzhaeva LA, Mapes RH, Mutvei H. 2010 Evolutionary patterns of Carboniferous coleoid cephalopods based on their diversity and morphological plasticity. In *Cephalopods present and past* (eds K Tanabe, Y Shigeta, H Hirano), pp. 171–180. Tokyo, Japan: Tokai University Press.
10. Strugnell J, Norman M, Jackson J, Drummond AJ, Cooper A. 2005 Molecular phylogeny of coleoid cephalopods (Mollusca: Cephalopoda) using a multigene approach; the effect of data partitioning on resolving phylogenies in a Bayesian framework. *Mol. Phylogenet. Evol.* **37**, 426–441. (doi:10.1016/j.ympev.2005.03.020)
11. Strugnell J, Jackson J, Drummond AJ, Cooper A. 2006 Divergence time estimates for major cephalopod groups: evidence from multiple genes. *Cladistics* **22**, 89–96. (doi:10.1111/j.1096-0031.2006.00086.x)
12. Strugnell JM, Rogers AD, Prodöhl PA, Collins MA, Allcock AL. 2008 The thermohaline expressway: the Southern Ocean as a centre of origin for deep-sea octopuses. *Cladistics* **24**, 853–860. (doi:10.1111/j.1096-0031.2008.00234.x)
13. Cooper A, Fortey R. 1998 Evolutionary explosions and the phylogenetic fuse. *Trends Ecol. Evol*. **13**, 151–156. (doi:10.1016/s0169-5347(97)01277-9)
14. Donoghue PC, Smith MP (eds). 2003 *Telling the evolutionary time: molecular clocks and the fossil record*. Boca Raton, FL: CRC Press. (doi:10.1201/b12432)
15. Smith MR, Caron JB. 2010 Primitive soft-bodied cephalopods from the Cambrian. *Nature* **465**, 469–472. (doi:10.1038/nature09068)
16. Smith MR. 2013 Nectocaridid ecology, diversity, and affinity: early origin of a cephalopod-like body plan. *Paleobiology* **39**, 297–321. (doi:10.1666/12029)
17. Vinther J *et al*. 2025 A fossilized ventral ganglion reveals a chaetognath affinity for Cambrian nectocaridids. *Sci. Adv.* **11**, eadu6990. (doi:10.1126/sciadv.adu6990)
18. Fuchs D. 2006 Fossil erhaltungsfähige merkmalskomplexe der Coleoidea (Cephalopoda) und ihre phylogenetische Bedeutung. *Berl. Palaobiologische Abh.* **8**, 1–122.
19. Fuchs D. 2020 Part M, chapter 23G: systematic descriptions: Octobrachia. *Treatise Online* **138**, 1–52. (doi:10.17161/to.vi.14661)
20. Fuchs D, Bracchi G, Weis R. 2009 New octopods (Cephalopoda: Coleoidea) from the late Cretaceous (Upper Cenomanian) of Hâkel and Hâdjoula, Lebanon. *Palaeontology* **52**, 65–81. (doi:10.1111/j.1475-4983.2008.00828.x)
21. Gibson R, Atkinson R, Gordon J. 2006 Taxonomy, ecology and behaviour of the cirrate octopods. *Oceanogr. Mar. Biol*. **44**, 277–322.
22. Nixon M. 2011 Part M, chapter 3: anatomy of recent forms. *Treatise Online* **17**, 1–52. (doi:10.17161/to.v0i0.4087)
23. Rogers CS, Astrop TI, Webb SM, Ito S, Wakamatsu K, McNamara ME. 2019 Synchrotron X-ray absorption spectroscopy of melanosomes in vertebrates and cephalopods: implications for the affinity of *Tullimonstrum*. *Proc. R. Soc. B* **286**, 20191649. (doi:10.1098/rspb.2019.1649)
24. Gabbott SE, Donoghue PCJ, Sansom RS, Vinther J, Dolocan A, Purnell MA. 2016 Pigmented anatomy in Carboniferous cyclostomes and the evolution of the vertebrate eye. *Proc. R. Soc. B* **283**, 20161151. (doi:10.1098/rspb.2016.1151)
25. Clements T, Dolocan A, Martin P, Purnell MA, Vinther J, Gabbott SE. 2016 The eyes of *Tullimonstrum* reveal a vertebrate affinity. *Nature* **532**, 500–503. (doi:10.1038/nature17647)

26. Roy A, Rogers CS, Clements T, Pittman M, Habimana O, Martin P, Vinther J. 2020 Fossil microbodies are melanosomes: evaluating and rejecting the 'fossilized decay-associated microbes' hypothesis. *Bull. Am. Mus. Nat. Hist.* **440**, 251–276.
27. McCoy VE, Wittry J, Sadabadi H, Mayer P. 2023 A reappraisal of *Nemavermes mackeei* from the Mazon Creek fossil site expands Carboniferous cyclostome diversity. *J. Paleontol*. **97**, 1116–1132. (doi:10.1017/jpa.2023.72)
28. Sutton M, Perales-Raya C, Gilbert I. 2016 A phylogeny of fossil and living neocoleoid cephalopods. *Cladistics* **32**, 297–307. (doi:10.1111/cla.12131)
29. Klug C, Landman NH, Fuchs D, Mapes RH, Pohle A, Guériau P, Reguer S, Hoffmann R. 2019 Anatomy and evolution of the first Coleoidea in the Carboniferous. *Commun. Biol*. **2**, 280. (doi:10.1038/s42003-019-0523-2)
30. Whalen CD, Landman NH. 2022 Fossil coleoid cephalopod from the Mississippian Bear Gulch Lagerstätte sheds light on early vampyropod evolution. *Nat. Commun*. **13**, 1107. (doi:10.1038/s41467-022-28333-5)
31. Klug C *et al*. 2023 Revisiting the identification of *Syllipsimopodi bideni* and timing of the decabrachian-octobrachian divergence. *Nat. Commun*. **14**, 8094. (doi:10.1038/s41467-023-42842-x)
32. Verhoeff TJ. 2023 The molecular phylogeny of cirrate octopods (Cephalopoda: Octopoda: Cirrata) using COI and 16S sequences. *Folia Malacol*. **31**, 175–196. (doi:10.12657/folmal.031.026)
33. Fuchs D, Schweigert G. 2018 First middle–late jurassic gladius vestiges provide new evidence on the detailed origin of incirrate and cirrate octopuses (Coleoidea). *PalZ* **92**, 203–217. (doi:10.1007/s12542-017-0399-8)
34. Fuchs D, Iba Y, Heyng A, Iijima M, Klug C, Larson NL, Schweigert G. 2020 The Muensterelloidea: phylogeny and character evolution of mesozoic stem octopods. *Pap. Palaeontol.* **6**, 31–92. (doi:10.1002/spp2.1254)
35. Baird GC, Sroka SD, Shabica CW, Kuecher GJ. 1986 Taphonomy of middle Pennsylvanian Mazon Creek area Fossil Localities, Northeast Illinois: significance of exceptional fossil preservation in syngenetic concretions. *Palaios* **1**, 271–285. (doi:10.2307/3514690)
36. Johnson RG, Richardson ES. 1966 A Remarkable Pennsylvanian fauna from the Mazon Creek Area, Illinois. *J. Geol.* **74**, 626–631. (doi:10.1086/627194)
37. Saunders WB, Richardson ES. 1979 Middle Pennsylvanian (Desmoinesean) Cephalopoda of the Mazon Creek Fauna, Northeastern Illinois. In *Mazon creek fossils* (ed. MH Nitecki), pp. 333–359. London, UK: Academic Press. (doi:10.1016/b978-0-12-519650-5.50020-5)
38. Kluessendorf J. 1997 Cephalopods. In *Richardson's guide to the fossil fauna of the Mazon Creek* (eds CW Shabica, AA Hays), pp. 30–34. Chicago, IL: Northeastern Illinois University.
39. Sutton MD, Garwood RJ, Siveter DJ, Siveter DJ. 2012 SPIERS and VAXML: a software toolkit for tomographic visualisation and a format for virtual specimen interchang. *Palaeontol. Electron* **15/5T**, 14. (doi:10.26879/289)
40. Schöder S *et al*. 2024 Heritage research at the PUMA beamline. *Appl. Phys. A* **130**, 848. (doi:10.1007/s00339-024-08091-5)
41. Leclercq N, Berthault J, Langlois F, Le S, Poirier S, Bisou J, Blache F, Medjoubi K, Mocuta C. 2015 October. Flyscan: a fast and multi-technique data acquisition platform for the SOLEIL beamlines. In *Proc. of the 15th Int. Conf. on Accelerator and Large Experimental Physics Control Systems (ICALEPCS)*, pp. 826–829. IAEA. https://accelconf.web.cern.ch/ICALEPCS2015.
42. Tischlinger H. 2001 Die oberjurassischen Plattenkalke von Daiting. In *Klassische fundstellen der palaontologie, Bd. IV* (ed. WK Weidert), pp. 139–151. Korb, Germany: Goldschneck Verlag.
43. Haug C, Haug JT, Waloszek D, Maas A, Frattigiani R, Liebau S. 2009 New methods to document fossils from lithographic limestones of southern Germany and Lebanon. *Palaeontol. Electron.* **12**, 12.
44. Haug JT *et al*. 2011 Autofluorescence imaging, an excellent tool for comparative morphology. *J. Microsc*. **244**, 259–272. (doi:10.1111/j.1365-2818.2011.03534.x)
45. Kaye TG, Falk AR, Pittman M, Sereno PC, Martin LD, Burnham DA, Gong E, Xu X, Wang Y. 2015 Laser-stimulated fluorescence in paleontology. *PLoS One* **10**, e0125923. (doi:10.1371/journal.pone.0125923)
46. Doguzhaeva LA, Mapes RH, Mutvei H. 2007 A Late carboniferous coleoid cephalopod from the Mazon Creek Lagerstätte (USA), with a Radula, Arm Hooks, Mantle Tissues, and Ink. In *Cephalopods present and past: new insights and fresh perspectives* (eds NH Landman, RA Davis, RH Mapes), pp. 121–143. Dordrecht, The Netherlands: Springer. (doi:10.1007/978-1-4020-6806-5_6)
47. Klug C, Pohle A, Roth R, Hoffmann R, Wani R, Tajika A. 2021 Preservation of nautilid soft parts inside and outside the conch interpreted as central nervous system, eyes, and renal concrements from the Lebanese Cenomanian. *Swiss J. Palaeontol*. **140**, 1–11. (doi:10.1186/s13358-021-00229-9)
48. Solem A, Richardson ES. 1975 *Paleocadmus*, a nautiloid cephalopod radula from the Pennsylvanian Francis Creek Shale of Illinois. *Veliger* **17**, 233–242.
49. Yochelson EL, Richardson ES. 1979 Polyplacophoran molluscs of the Essex fauna (middle Pennsylvanian, Illinois). In *Mazon creek fossils*, pp. 321–332. New York, NY: Academic Press. (doi:10.1016/b978-0-12-519650-5.50019-9)
50. Kruta I, Landman NH, Tanabe K. 2015 Ammonoid radula. In *Ammonoid paleobiology: from anatomy to ecology* (eds C Klug, D Korn, K De Baets, I Kruta, RH Mapes), pp. 485–505. Dordrecht, The Netherlands: Springer. (doi:10.1007/978-94-017-9630-9_11)
51. Mejia S. 2018 *Cephalopod Radula under the SEM; Homodont Radula*. Cephalopod Morphology Studies. See https://cephalopodceramist.wordpress.com/2018/10/24/homodont-radula/ (accessed March 2025).
52. O'Shea S, Lu CC. 2002 A new species of *Luteuthis* (Mollusca: Cephalopoda: Octopoda: Cirrata) from the South China Sea. *Zool. Stud. TAIPEI* **41**, 119–126.
53. Collins MA. 2003 The genus *Grimpoteuthis* (Octopoda: Grimpoteuthidae) in the north-east Atlantic, with descriptions of three new species. *Zool. J. Linn. Soc*. **139**, 93–127. (doi:10.1046/j.1096-3642.2003.00074.x)
54. Guerra A, Villanueva R, Nesis KN, Bedoya J. 1998 Redescription of the deep-sea cirrate octopod *Cirroteuthis magna* Hoyle, 1885, and considerations on the genus *Cirroteuthis* (Mollusca: Cephalopoda). *Bull. Mar. Sci*. **63**, 51–81.
55. Voss NA, Vecchione M, Toll RB, Sweeney MJ. 1988 Systematics and biogeography of cephalopods. *Smithsonian Contrib. Zool* **586**, 1–276.
56. Runnegar B. 2011 Once again: is *Nectocaris pteryx* a stem-group cephalopod? *Lethaia* **44**, 373–373. (doi:10.1111/j.1502-3931.2011.00296.x)
57. Mazurek D, Zatoń M. 2011 Is *Nectocaris pteryx* a cephalopod? *Lethaia* **44**, 2–4. (doi:10.1111/j.1502-3931.2010.00253.x)
58. Sallan LC, Coates MI. 2014 The long-rostrumed elasmobranch *Bandringa* Zangerl, 1969, and taphonomy within a Carboniferous shark nursery. *J. Vertebr. Paleontol.* **34**, 22–33. (doi:10.1080/02724634.2013.782875)
59. Plotnick RE, Young GA, Hagadorn JW. 2023 An abundant sea anemone from the Carboniferous Mazon Creek Lagerstätte, USA. *Pap. Palaeontol*. **9**, e1479. (doi:10.1002/spp2.1479)
60. Schiffbauer J, Baird GC, Huntley JW, Selly T, Shabica CW, Laflamme M, Muscente AD. 2025 283,821 concretions, how do you measure the Mazon Creek? Assessing the paleoenvironmental and taphonomic nature of the Braidwood and Essex assemblages. *Paleobiology* **51**, 488–506. (doi:10.1017/pab.2025.10045)
61. Clements T, Colleary C, De Baets K, Vinther J. 2017 Buoyancy mechanisms limit preservation of coleoid cephalopod soft tissues in Mesozoic Lagerstätten. *Palaeontology* **60**, 1–14. (doi:10.1111/pala.12267)
62. Kear AJ, Briggs DE, Donovan DT. 1995 Decay and fossilization of non-mineralized tissue in coleoid cephalopods. *Palaeontology* **38**, 105–132.

63. Reyment RA. 2008 A review of the post-mortem dispersal of cephalopod shells. *Palaeontol. Electron*. **11**, 1–13.
64. Wani R, Gupta NS. 2015 Ammonoid taphonomy. In *Ammonoid paleobiology: from macroevolution to paleogeography* (eds C Klug, D Korn, K De Baets, I Kruta, RH Mapes), pp. 555–598. Dordrecht, The Netherlands: Springer. (doi:10.1007/978-94-017-9633-0_20)
65. Yacobucci MM. 2018 Postmortem transport in fossil and modern shelled cephalopods. *PeerJ* **6**, e5909. (doi:10.7717/peerj.5909)
66. Wani R, Kase T, Shigeta Y, Ocampo RD. 2005 New look at ammonoid taphonomy, based on field experiments with modern chambered nautilus. *Geology* **33**, 849–852. (doi:10.1130/g21712.1)
67. Wani R. 2007 How to recognize *in situ* fossil cephalopods: evidence from experiments with modern *Nautilus*. *Lethaia* **40**, 305–311. (doi:10.1111/j.1502-3931.2007.00029.x)
68. Cherns L, Spencer ART, Rahman IA, Garwood RJ, Reedman C, Burca G, Turner MJ, Hollingworth NTJ, Hilton J. 2022 Correlative tomography of an exceptionally preserved Jurassic ammonite implies hyponome-propelled swimming. *Geology* **50**, 397–401. (doi:10.1130/g49551.1)
69. Klug C, Schweigert G, Tischlinger H, Pochmann H. 2021 Failed prey or peculiar necrolysis? Isolated ammonite soft body from the Late Jurassic of Eichstätt (Germany) with complete digestive tract and male reproductive organs. *Swiss J. Palaeontol*. **140**, 1–14. (doi:10.1186/s13358-020-00215-7)
70. Donovan DT, Fuchs D. 2016 Part M, chapter 13: fossilized soft tissues in Coleoidea. *Treatise Online* **73**, 1–30.
71. Clements T, Purnell MA, Gabbott S. 2022 Experimental analysis of organ decay and pH gradients within a carcass and the implications for phosphatization of soft tissues. *Palaeontology* **65**, e12617. (doi:10.1111/pala.12617)
72. Briggs DEG, Wilby PR. 1996 The role of the calcium carbonate-calcium phosphate switch in the mineralization of soft-bodied fossils. *J. Geol. Soc*. **153**, 665–668. (doi:10.1144/gsjgs.153.5.0665)
73. Sagemann J, Bale SJ, Briggs DEG, Parkes RJ. 1999 Controls on the formation of authigenic minerals in association with decaying organic matter: an experimental approach. *Geochim. Et Cosmochim. Acta* **63**, 1083–1095. (doi:10.1016/s0016-7037(99)00087-3)
74. Lin CY, Turchyn AV, Krylov A, Antler G. 2020 The microbially driven formation of siderite in salt marsh sediments. *Geobiology* **18**, 207–224. (doi:10.1111/gbi.12371)
75. Clements T *et al*. 2026 CT Data for: Synchrotron data reveal nautiloid-characters in *Pohlsepia mazonensis*, refuting a Palaeozoic origin for octobrachians. [Dataset]. Dryad Digital Repository. (doi:10.5061/dryad.n8pk0p38p)
76. Clements TG *et al*. 2026 Supplementary material from: Synchrotron data reveal nautiloid-characters in Pohlsepia mazonensis, refuting a Palaeozoic origin for octobrachians. Figshare. (doi:10.6084/m9.figshare.c.8388504)